

# MICROPHONICS IN CW TESLA CAVITIES AND THEIR COMPENSATION WITH FAST TUNERS\*

A. Neumann<sup>†</sup>, W. Anders, J. Knobloch, O. Kugeler, BESSY, Berlin, Germany

## Abstract

Superconducting linac cavities of single pass Free Electron Lasers or Energy Recovery Facilities have a very low or near zero beamloading and are thus operated at a high quality factor with a narrow RF resonance, respectively. Following the phase and amplitude stability of the RF field is very easily degraded by any kind of mechanical detuning. In CW operation microphonics is the main error source for cavity detuning. To achieve high field stabilities in the regime of  $0.02^\circ$  in phase and  $1 \cdot 10^{-3}$  down to  $1 \cdot 10^{-4}$  in amplitude a fast tuning system is mandatory to compensate the detuning. In this paper the microphonics detuning measured at HoBiCaT will be shown and analyzed with respect to a detuning controller application. The controller design is given by a combination of a feedback and adaptive feedforward approach based on fast piezo tuners implemented in the Saclay coarse tuner designs. It will be shown, that at 1.8 K and loaded quality factors between  $3 \cdot 10^7$ - $1 \cdot 10^8$  a compensation of a least a factor of two up to seven is achievable.

## INTRODUCTION

Present single pass Free Electron Laser (FEL) Linear Accelerators (linac) as of the BESSY-FEL [1] or Energy Recovery Linacs (ERL) like the Cornell ERL or the 4GLS at Daresbury ([2] and [3]) require a precise synchronization of the RF field with the electron beam and a high stability of the accelerating field. RF control simulations in [4] show, that a field stability down to  $0.02^\circ$  is required to achieve the strict boundaries set by the seeded FEL process for the beam stability. Many of these projects will use a linac based on superconducting RF TESLA technology.

The very low or near zero beamloading allows to operate the cavities at a high loaded quality factor for optimized power transfer to the beam. This leads to a narrow cavity bandwidth of the order of tens of Hertz. Already mechanical shifts of the order of nm will detune the cavity by sub-Hertz to Hertz degrading the field stability. There are several reasons to determine the nature and amount of mechanical detuning in CW-driven cavities and to find countermeasures against it:

- The needed forward power to be supplied to the cavity to maintain a constant RF field amplitude is given by

Equation 1:

$$P_f = \frac{V_{cav}^2}{4 \left(\frac{r}{Q}\right) Q_L} \cdot \left( \left( 1 + \frac{\left(\frac{r}{Q}\right) Q_L I_b}{V_{cav}} \cos(\Phi_b) \right)^2 + \left( \left( \frac{\Delta f}{f_{1/2}} \right) + \frac{\left(\frac{r}{Q}\right) Q_L I_b}{V_{cav}} \sin(\Phi_b) \right)^2 \right) \quad (1)$$

Here  $Q_L$  is the loaded quality factor,  $V_{cav}$  the cavity field amplitude,  $f_{1/2}$  the half-bandwidth,  $I_b$  the RF component of the beam current and  $\Phi_b$  the beam phase. Assuming a very low beamloading or beam current, respectively the amount of power evolves with the detuning over the cavity bandwidth squared. To stabilize the RF field against the detuning effect a LLRF controller will increase the power to keep the field level. But as the RF power may be limited to some kW strong detuning effects may lead to ponderomotive instabilities driven by the dynamic Lorentz force detuning or degrade the field stability above the required limit.

- In general the feedback gain of an LLRF control might be limited by measurement noise as e.g. phase noise of the RF reference system. To achieve the strict boundary conditions for the acceleration in an ERL or single pass FEL linac, it is thus of great importance to compensate for the main error source.

In CW-driven machines it is given by mechanical background vibrations, general referred to as microphonics.

At the HoBiCaT test facility TESLA cavities have been characterized in CW mode in cryo-module like conditions to measure the amount of microphonics to be expected for linac operation. The nature of this detuning effect has been characterized, the mechanisms driving the effective detuning have been partly tracked down and fast tuners based on the piezo-electric effect have been evaluated with respect to a detuning controller application. The possible sources for a CW cavity detuning are shown in Figure 1.

It will be shown, that for a typical microphonics spectrum, which was obtained at HoBiCaT and the boundary conditions given by the transfer function between the piezo tuner and the cavity's RF response a combination of a feedback solution and an adaptive feedforward compensation is suitable to reduce the detuning to the resolution limit of the tuner.

\* Work partially supported by the EU Commission in the sixth framework programme, contract no 011935 EURO-FEL-DS5, BMBF and Land Berlin.

<sup>†</sup> Axel.Neumann@bessy.de

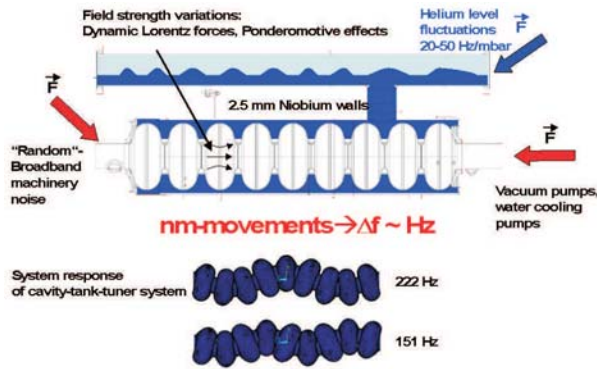


Figure 1: Possible sources for microphonics detuning for a CW driven cavity.

## MEASUREMENT SETUP

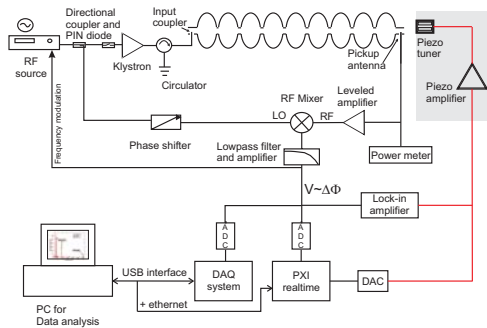


Figure 2: Measurement setup at the HoBiCaT test facility.

Figure 2 shows the measurement setup at the Ho-BiCaT [5] test facility. The cavity is driven by an Rhode&Schwartz SML02 RF source<sup>1</sup>. The input RF signal to the klystron can be damped by a programmable attenuator and switched between CW or pulsed mode. Furthermore the coupling strength of the forward power wave can be varied by changing the input couplers penetration depth's into the cavity beam line and by changing the phase of the standing wave between circulator and coupler by a three-stub-tuner. The obtained coupling range expressed in loaded quality factor  $Q_L$  is between  $3 \cdot 10^7$  up to  $1 \cdot 10^{10}$ . The field stored in the cavity is measured via a weakly coupled pick-up antenna and compared to the reference source at a mixer to extract the cavity detuning information. To suppress any amplitude modulation the pick-up signal is kept at a constant amplitude by a phase stable limiting amplifier. The phase of the reference source may be adapted by a programmable phase shifter. The detuning signal of the phase detector (mixer) is amplified by a low noise device including a lowpass filter. This signal is sampled by a

<sup>1</sup>For an improved phase accuracy it will be replaced in the near future by a low phase noise reference source

data acquisition system with a resolution of 18 Bit at rates between 1.0-5.0 kHz, which covers the typical microphonics detuning frequency spectrum sufficiently. Aliasing of higher frequency components have not been observed.

As a closed loop phase-locked-loop (PLL) setup varies the measured detuning spectrum depending on the frequency by its transfer function, most microphonics detuning measurements have been performed open loop. The loaded quality factors have been between  $3 \cdot 10^7$  up to  $1 \cdot 10^8$  being related to cavity half-bandwidths  $f_{1/2}$  of 21.7-6.5 Hz. In open loop mode it has therefore been more straightforward to find a calibration factor for the RF field phase detection at the mixer.

The piezo-to-RF detuning transfer functions have been recorded by a SR 850 lock-in amplifier in PLL closed loop mode. The loop gain has been optimized to compensate for the filtering effect of the cavity transfer function by still keeping an acceptable detuning resolution (Hz/V).

## MICROPHONICS DETUNING MEASUREMENTS AND ANALYSIS

Some of the results presented here have been already shown in [6] and [7]. Figure 3 depicts a typical example of the integrated detuning spectra for two different cavities with the same tuner system installed (Saclay I). Taking all measurements at HoBiCaT into account the total rms detuning measured varied between 1-5 Hz rms, being mostly gaussian distributed, but for some examples showing a bimodal, sinusoidal distribution. About 50-60% of the total detuning has been related to liquid helium level fluctuations in the two-phase line of the cryo-unit. The modulating frequencies of this effect are below 1 Hz. The static pressure dependance has been determined to 50-55 Hz/mbar. This has been proven by calculating the cross-correlation

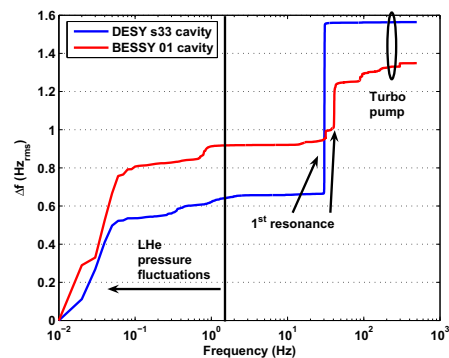


Figure 3: Integrated microphonics spectrum of two TESLA cavities with the same tuner systems installed (Saclay I). The spectra seem to be dependent on the cavity and are governed by helium pressure fluctuations, excited mechanical resonances of the cavity-tuner system and deterministic external sources like the isolation vacuum turbo pump at 300 Hz.

between the pressure sensor signal and the RF detuning

signal. It is even more obvious when filtering the detuning data by software to the frequency range of the helium level fluctuations. The lower plot of Figure 4 shows the correlation of the detuning signals of the two cavities installed in HoBiCaT to the pressure variations. It is governed by the slow helium drift in the hundredth Hertz regime and a 0.8 Hz contribution. The helium pressure variation is also the only source for a correlation of microphonics detuning between the two cavities installed at that time in the cryostat, as given by the cross-correlation between both detuning signals in the upper plot of Figure 4. For the correlation measurements both cavities were driven by the same reference, i.e. tuned to the same RF eigenmode frequency.

The microphonics spectrum is furthermore dominated by one strong line, which is as follows a nearly constantly excited mechanical resonance. Most likely it is a transverse mode according to [8] and [9]. Some further lines with negligible integral detuning are given by deterministic external error sources as the isolation vacuum turbo pump and water cooling pumps (not marked in Figure3). To analyze what

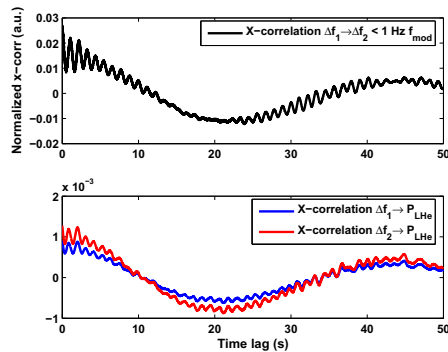


Figure 4: Correlated microphonics between two cavities in the HoBiCaT cryostat. The correlation occurs in the low frequency part of the spectrum only, which is caused by helium level fluctuations. The upper plot shows the cross-correlation between the two lowpass filtered cavity detuning signals. The cross-correlation of the detuning signals to the helium pressure signal is shown in the lower plot.

causes the dominant lines in the microphonics spectrum an autocorrelation analysis is useful to characterize the nature of the process driving the detuning. Shown in Figure 5 is the measured detuning and the autocorrelation of this signal. It shows the behavior of an excited second order system, which damps down and starts to be excited again some hundred milliseconds later. This hints at band-limited random background noise being the source for the excitation of this mode. The quality factor of this mode is about 20-30, which later has been proven by the mode obtained from a fit to the piezo-to-RF detuning transfer function.

### Long-term measurements

Even if the usual rms detuning should be very low, long-term observation over several hours have to show, what

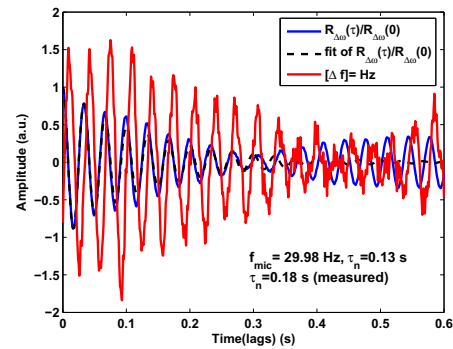


Figure 5: Autocorrelation analysis of microphonics detuning. The autocorrelation (blue line) has been calculated from the measured detuning (red line). It shows the decay of an excited second order system. The decay time has been determined experimentally and by fitting the expected second order behavior (black line).

kind of peak detuning events may happen. Additionally it is of interest how often they may happen and what triggers such an event. For such a measurement the detuning has been recorded over 14 hours in data sets of 100 seconds. Should the peak detuning within such a data set exceed the current absolute maximum, the data set is saved to the memory. Constantly the rms detuning of each set is filled into an histogram. Slow drifts below 0.01 Hz, most likely caused by changes in the tuner temperature, are compensated by the piezo tuner to keep the cavity on resonance. The peak events showed to be 12-17 standard deviations above the usual rms detuning of 1-1.5 Hz and are occurring about 10 times in a period of 12 hours. They are mostly caused by an increased excitation of the first resonance and more seldom by thermo-acoustic helium pressure fluctuations.

### Time-frequency analysis

As the autocorrelation already showed, it may be expected, that the spectral components of the detuning are not invariant with time. This is an important feature to determine, as strong spectral variations would inhibit the use of a pure feedforward controller. Figure 6 displays the wavelet transform of the detuning signal by Morlet wavelets. In a resolution bandwidth of 3 Hz the excited eigenmode varies its contribution from 0.2 up to 10 Hz on a sub-second timescale. Not shown is the variation of the helium pressure induced low-frequency detuning. This showed to be of a more random nature sometimes showing sinusoidal strong pressure induced fluctuations, which may be caused by thermo-acoustic effects. The occurrence of such a high pressure variation also seems to be of random nature.

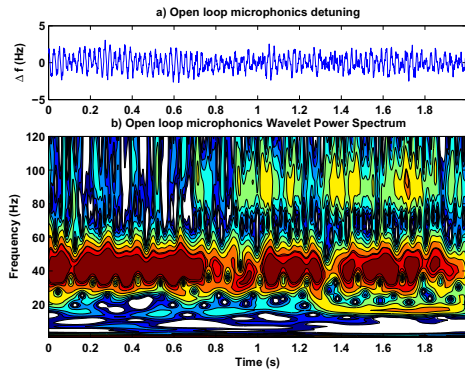


Figure 6: Time-frequency analysis of open loop detuning data by Morlet wavelets. The upper plot shows the time domain detuning signal, the lower plot the time-frequency map obtained by the Wavelet transformation. In a bandwidth of about 3 Hz the first resonance detuning contribution varies from 0.2 up to 10 Hz.

## FAST TUNING SYSTEMS FOR CONTROL

To control the fast detuning the Saclay I and II coarse tuning systems are equipped with piezo-based tuning devices. Their extensive characterization is described in [10]. At HoBiCaT they have been adapted and partly modified to meet the requirements for CW operation and detuning control. The following properties are important for an effective detuning control system:

- Achieve a displacement of several  $\mu\text{m}$  at temperatures below 2-20 K related to a tuning range of several hundred Hertz. This is important to also cover static Lorentz force detuning effects and motor tuner hysteresis, which showed to be between 30-50 Hz [11].
- Work against a stiff and massive system related to a blocking force of several kN and sustain a radioactive environment in case of beam loss or field emission of the cavity.
- A good resolution of sub-Hertz to even counteract very low microphonics contributions in a spectrum
- A flat response for the frequency range of interest up to  $\sim\text{kHz}$ , which is equivalent to having a fast response time or low group delay of the tuner

Figure 7 shows a typical piezo-to-RF detuning transfer function for the Saclay I tuner with an improved stiffness of the piezo frame. It displays the first low resonance at 30 Hz, which is a pair of a resonance-antiresonance. This first resonance position is independent of the tuner system and a result of the cavity mechanics and presumably the welding into the helium vessel. But it has been observed, that the Saclay II tuner leads to a more complex substructure of the first resonance. The resonance-antiresonance appears as a double pair configuration.

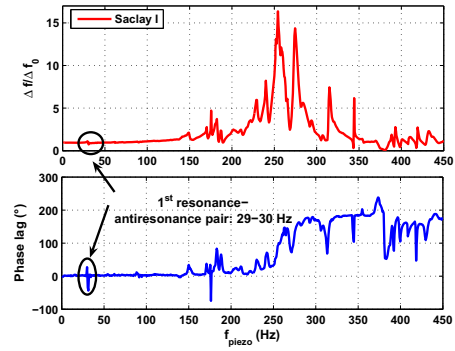


Figure 7: Piezo-to-RF detuning transfer function of a TESLA cavity taken with the SR 850 lock-in amplifier in closed loop PLL mode with the Saclay I tuner installed.

The piezo couples clearly to several mechanical modes of the cavity-tuner system. Some negative dips below the general excitation level of the tuner occur. There the cavity responds with a less effective detuning, maybe in a mode, which has no influence on the resonance frequency of the  $\text{TM}_{010}$  mode. The resolution of the piezo tuner, given by the hysteresis, is about 0.1-0.2 Hz and depends on the tuners overall stiffness. The group delays, extracted from the slope of the phase response of the transfer function varied between 0.1-1.2 ms and is also critically depending on the stiffness of the setup and the pre-load onto the piezos.

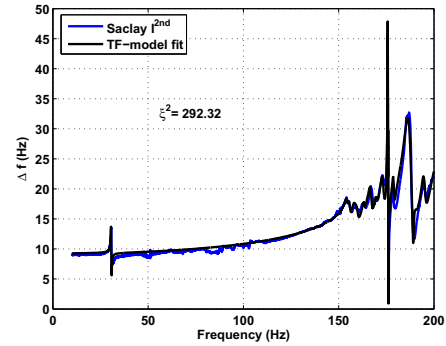


Figure 8: Fit of a subrange of the transfer function by a sum of second order systems. For this range already 20 modes were used to achieve this result.

According to [12] it is possible to fit the transfer function by a set of second order systems convolved by the group delay and a dc response containing the higher modes response at lower frequencies. The individual modes are given by:

$$H_k(s) = \frac{\omega_k^2 M_k}{s^2 + 2\xi_k \omega_k s + \omega_k^2}, \quad (2)$$

with  $s = i \cdot \omega$ ,  $\xi_k = 2\omega_{1/2,k}/\omega_k = 0.5/Q_{m,k}$  and  $M_k$  is given by the steady state solution of the second order system as  $\pm 2\xi_k \Delta f_k$ .  $\Delta f_k$  is the measured amplitude response of the transfer function. The global phase slope due to the



group delay of the acoustic wave in the tuner medium is:

$$H_{delay}(s) = \exp(-T_{delay} \cdot s). \quad (3)$$

$T_{delay}$  is the measured group delay. To account for the lower frequency and DC contribution of modes beyond the measurement range a kind of low-pass transfer function may be added:

$$H_0(s) = \frac{M_0}{\tau s + 1}, \quad (4)$$

where  $\tau$  relates to the cut-off frequency of the total measurement setup and is around 1.0 kHz. The total transfer function model thus is given by Equation 5:

$$H(s) = \left( H_0(s) + \sum_{k=1}^N H_k(s) \right) \cdot H_{delay}(s). \quad (5)$$

The result for the frequency range, where most microphonics detuning happens, is given in 8. Already for that small portion of the transfer function 20 modes have been used for the fitting, that 63 fit parameters had to be optimized. For the Saclay II tuner even double the number of modes were needed.

It is essential due to stability reasons to have an exact mathematical model for the complex system to be controlled. That means for the controller to choose a design, where a look-up table based solution would be sufficient.

## COMPENSATION STRATEGY: A COMBINED FEEDBACK AND ADAPTIVE FEEDFORWARD

The structure of the piezo-to-RF detuning transfer function and the typical microphonics spectrum allow for a two-folded approach for a compensation scheme. The solution is to split the measured detuning signal in a lowpass filtered low-frequency path and a second path for an adaptive feedforward scheme. The setup of the controller is given in Figure 9. For prototyping it has been programmed on a National Instruments realtime system.

The measured microphonics is in principle some unknown external error source convolved by an unknown transfer function. Excited mechanical modes or constant oscillations outside the bandwidth of such a mode may be compensated, if they are visible in the RF detuning spectrum and there is an effective non-zero excitation by the piezo tuner at that frequency.

To cover the random helium pressure oscillations caused detuning the sampled phase error signal is split into two paths. The first path is filtered by a first order lowpass filter with a 3 dB cutoff frequency of 1.4 Hz and further processed by a proportional-integral controller. This signal modulates the piezo via the amplifier to compensate for the slow resonance drifts.

The second signal path is to compensate the contribution of one or even more excited mechanical resonances being based on an adaptive feedforward algorithm, which can be

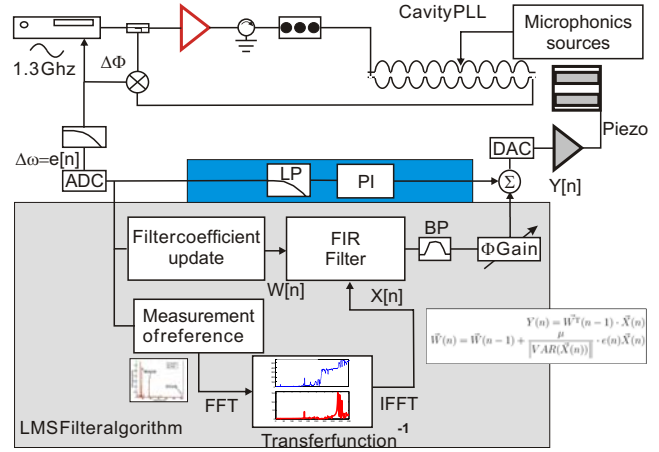


Figure 9: Setup of the combined detuning controller made up of a low-frequency proportional-integral feedback loop and an adaptive least-mean-square based FIR filter feedforward system.

found in the field of active noise control (ANC) [13]. A reference signal, which resembles the signal to be canceled, is altered by a finite-impulse-response filter (FIR) such, that it produces via the piezo-to-RF detuning transfer function a signal that negates the external microphonics to a minimum. The filter coefficients are constantly updated by the residual error according to the method of the steepest descent to converge to the local minimum solution.

For the RF cavity application that means, to provide the algorithm with a reference signal resembling the external microphonics. The option used here is to deconvolve the measured detuning with the transfer function to transform it from the cavity to the tuner side. A two seconds long reference signal is continuously played and the current subrange in time is multiplied with the filter coefficients. The resulting control signal is filtered by a narrow bandpass filter to avoid excitation of neighboring modes. Programmable gain and phase shifters allow to alter the signal further to achieve a compensation. Each time step the filter coefficients are updated by the least-mean-square (LMS) algorithm involving the current error signal. The final feedforward algorithm is given by:

$$y[n] = H_{ext}z[n] - H_{cav}\vec{w}^T[n] \cdot \vec{x}[n], \quad (6)$$

$$e[n] = y[n] - d[n], \quad (7)$$

$$\vec{w}[n+1] = \vec{w}[n] - \mu \frac{e[n]\vec{x}[n]}{\beta + \vec{x}^T[n] \cdot \vec{x}[n]}. \quad (8)$$

Here  $y[n]$  is the controller output at time  $n \cdot T_{sample}$  given by the sum of the external detuning  $H_{ext}z[n]$  and the reference signal  $\vec{x}[n]$  altered by the filter  $\vec{w}[n]$  and the piezo-to-RF detuning transfer function. The measured error of each time step is the difference of the residual detuning and a defined set point  $d[n]$ . The filter coefficients are updated according to the LMS algorithm including a variable update gain  $\mu$  and a small constant  $\beta$  to keep the algorithm

within the convergence radius defined by the variance of the reference signal and thus the detuning.

Thus any strong change of the microphonics with time may push the algorithm beyond the stability limits. To avoid this a constant update of the reference signal is mandatory.

### Detuning control results

For the following exemplary results the sampling rate has been 2.0 kHz and 400 filter coefficients were used for the calculations. The cavity half-bandwidth was 10.2 Hz and operated at 1.8 K.

Figure 10 shows the performance of the feedback path. The obtained residual detuning below 10 Hz follows the expected steady state error of a proportional controller  $1/(1 + K_P)$  with  $K_P$  the proportional feedback gain. To avoid overshoots of the controller, the integral part has been chosen very small. Any further controller has been turned off and the cavity is stabilized by the piezo feedback only. The saturation at higher gains may be explained by the limited resolution of the piezos and the accuracy of the measurement setup.

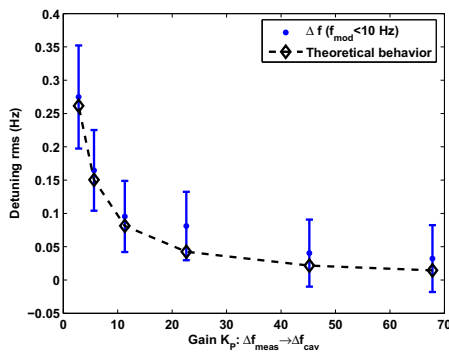


Figure 10: Residual detuning induced by helium pressure fluctuations controlled by the feedback path of the controller (blue dots). The error bars are given by variations of the corresponding open loop detuning. The black curve shows the theoretical compensation for a perfect feedback controller.

### Results of the combined controller

Figures 11- 13 show the performance of the combined controller for an open loop detuning of 2.5 Hz rms. It is compensated down to 0.89 Hz rms by the pure feedback control limiting the influence of the helium level variations and finally further suppressed to 0.36 Hz rms by applying the adaptive feedforward to the first mechanical resonance line. The peak detuning in the open loop case exceeds the half-bandwidth of the cavity, being here only 10.2 Hz. Due to the controller it has been limited down to 1.6 Hz. The measurements were done at comparable helium pressure variations. After finding the conditions for a stable feedforward control by fine adjustment of the output phase of the

controller signal, the FIR filter converged within one second to a stable solution. The algorithm kept stable for several hundred seconds without updating the reference signal. Following it is able to adapt to the variations of the detuning by the first mechanical resonance. In general it showed to be easier to compensate for strong detuning. This method reached its limitation in performance when the detuning was near the resolution of the piezo tuner.

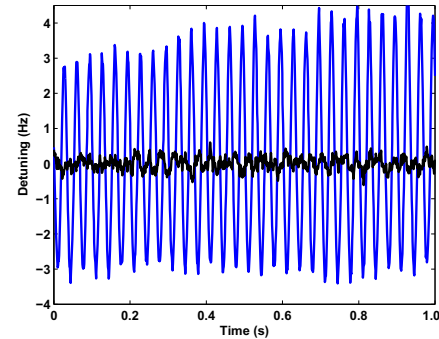


Figure 11: Time domain detuning for the open loop case (blue curve) and a combined feedback and feedforward controller (black curve) at a  $Q_L$  of  $6.4 \cdot 10^7$ .

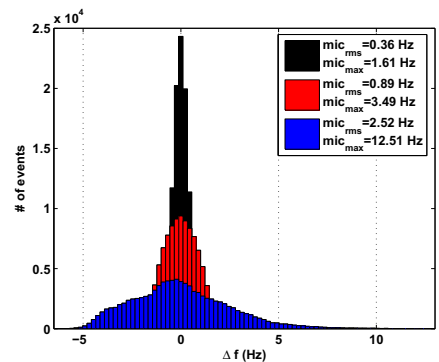


Figure 12: RMS detuning measured for 100 s for open loop (blue), feedback control only (red) and the combined controller (black).

Table summarizes the achieved compensation under different circumstances. The first two rows display results, where the residual detuning components in the spectrum were below the resolution of the piezo tuner. In the case of very high pressure variations, as shown in the third row, the effectiveness of the controller has been limited. At that time pressure variations of  $80 \mu\text{bar}$  occurred in contrast to the usual  $20\text{-}30 \mu\text{bar}$ . The last two rows show the achieved results at  $Q_L = 4 \cdot 10^7$  with the Saclay II tuner. There again the residual detuning error was given by the resolution of the tuner.

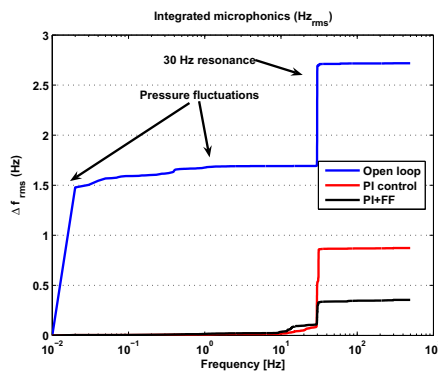


Figure 13: Integrated spectra of the open loop detuning (blue), the feedback controlled detuning (red) and the achieved residual detuning of the combined controller.

Table 1: Achieved phase stability in the compensation measurements. In the first three rows  $Q_L$  was  $6.4 \cdot 10^7$ , in the last two rows  $4 \cdot 10^7$ . The third row shows the result where high pressure variations occurred.

Open loop: $\sigma_f$ (Hz)	Closed loop: $\sigma_f$ (Hz)	$\sigma_\Phi$ (°)
1.7	0.45	2.52
2.52	0.36	2.01
3.8	1.7	9.43
5.3	0.8	2.82
0.74	0.37	1.32

## OUTLOOK

For an automated controller working in parallel with a LLRF control system, the reliability of the controller has to be improved further. Undesired crosstalk between both control systems has to be avoided and it has to be shown, that the detuning information can be extracted from the residual error signal of the LLRF controller.

A method to judge about the state of the feedforward path and if it converged to a stable solution has to be found. The recording of the filter coefficients and their derivative with time may serve as a diagnostic tool to judge if a convergence of the algorithm has been achieved.

## ACKNOWLEDGEMENTS

We would like to acknowledge the significant help from discussion with K. Jentsch and C. Albrecht from DESY and M. Luong, G. Devanz, E. Jacques and P. Bosland from CEA Saclay related to the design and installation of the tuning systems. Thanks for the support and operation of HoBiCaT to A. Frahm, M. Schuster, S. Klauke, P. Lauinger, D. Pflueckhahn, S. Rotterdam, Th. Westphal, H.G. Hoberg and K. Ludwig.

## REFERENCES

- [1] *The BESSY Soft X-ray Free Electron Laser*, TDR BESSY March 2004, eds.: D. Krämer, E. Jaeschke, W. Eberhardt, ISBN 3-9809534-0-8, BESSY, Berlin (2004)
- [2] G. H. Hoffstaetter, I.V. Bazarov, D. Bilderback, M. Billing, S. Gruner, M. Liepe, D. Sagan, C. Sinclair, R. Talman, and M. Tigner, "ERL Upgrade of an Existing X-ray Facility: CHSS at CESR", *Proc. of the 9<sup>th</sup> EPAC(2004)*, Lucerne, Switzerland, 2004.
- [3] 4GLS Conceptual Design Report, April 2006, found at: <http://www.4gls.ac.uk/documents.htm#CDR>
- [4] A. Neumann, J. Knobloch, "Cavity and Linac RF and detuning control simulations" *these proceedings*, Beijing, China, 2007.
- [5] J. Knobloch, W. Anders, J. Borninkhof, S. Jung, M. Martin, A. Neumann, D. Pflueckhahn, M. Schuster, "Status of the HoBiCaT Superconducting Cavity Test Facility at BESSY", *Proc. of the 9<sup>th</sup> EPAC(2004)*, Luzern, 2004.
- [6] O. Kugeler, W. Anders, J. Knobloch, A. Neumann, "Microphonics measurements in a cw-driven TESLA-type cavity" *Proc. of the 10<sup>th</sup> EPAC(2006)*, Edinburgh, 2006.
- [7] A. Neumann, W. Anders, S. Klauke, J. Knobloch, O Kugeler, M. Schuster, "Characterization of a piezo-based microphonics compensation system at HoBiCaT" *Proc. of the 10<sup>th</sup> EPAC(2006)*, Edinburgh, 2006.
- [8] A. Marziali, H.A. Schwetmann, W.W. Hansen, "Microphonic analysis of cryo-module design", *TESLA-report 1993-40*, Hamburg, 1993.
- [9] G. Devanz, M. Luong, A. Mosnier, "Numerical simulations of dynamic lorentz detuning of sc cavities", *Proc. of the 8<sup>th</sup> EPAC(2002)*, Paris, 2002.
- [10] O. Kugeler, A. Neumann, W. Anders, J. Knobloch, "Tuner", *these proceedings*, Beijing, China, 2007.
- [11] O. Kugeler, A. Neumann, W. Anders, J. Knobloch, "Measurement and compensation of microphonics in cw-operated TESLA-type cavities", *Proc. of the 41<sup>st</sup> Advanced ICFA beam dynamics workshop on Energy Recovery Linacs (ERL 2007)*, Daresbury, 2007.
- [12] M. Luong, P. Bosland, G. Devanz, E. Jacques, "Analysis of microphonic disturbance and simulation for feedback compensation", *Proc. of the 10<sup>th</sup> EPAC(2006)*, Edinburgh, 2006.
- [13] O. Tokhi, S. Veres, editors, "Active sound and vibration control, theory and application", *IEE control engineering series 62*, ISBN 3-9809534-0-8, London, 2002.